International Journal of Arrhythmia

CASE REPORT

Open Access

# Successful case of complex atrial flutter occurring in a patient with congenitally corrected transposition of the great arteries, aberrant left atrial appendage, and situs inversus

Feng Hu, Erpeng Liang, Lihui Zheng and Ligang Ding*

## Abstract

**Background:** Congenitally corrected transposition of great arteries (ccTGA) is a rare congenital cardiac defect with atrioventricular and ventriculoarterial discordance which leads to heart failure and limits patients' lifespan. The extremely aberrant cardiac structure makes electrophysiological procedure and radiofrequency ablation very difficult to be performed in such patients. Until now, there were only sporadical cases that have reported the successful ablation of atrial flutter in ccTGA patients.

**Case presentation:** We report a case of a 36-year-old male who was diagnosed with dextrocardia, atrial septal defect and congenitally corrected transposition of great arteries (ccTGA) at a young age and received atrial septal defect repair and morphological tricuspid valve plasty in 2014. As for reasons of heart failure and atrial flutter, he frequently suffered from progressively worsening dyspnea and recurrent episodes of palpitations. Cardiac anatomic imaging reconstruction before electrophysiological test revealed an unusually huge left atrial appendage in this patient. After high-density mapping of both right atrium and left atrium, activation mapping showed reentry circuit loops were located in left atrium. Successful ablation strategy was performed under the guidance of high-density mapping and entrainment.

**Conclusion:** This is a clinical case showing high-density mapping and successful ablation of a complex dual-loop atrial flutter in a patient with ccTGA and aberrant left atrial appendage. The successful procedure corroborates clinical utility of high-density mapping approach in the treatment of the patients with complex congenital heart disease accompanied by rapid arrhythmia, can be simpler, safer and more effective.

**Keywords:** Congenitally corrected transposition of great arteries, Congenital heart disease, Atrial flutter, High-density mapping, Radiofrequency ablation

## Background

Congenitally corrected transposition of great arteries (ccTGA) is a rare form of congenital heart disease (CHD) with the prevalence being less than 0.5% [1, 2]. Since many other associated anatomical defects, such as atrial septal defect, ventricular septal defect, pulmonary stenosis and abnormalities of the morphological tricuspid valve, occurred in the majority of ccTGA patients, surgical treatment was performed in quite a number of these patients [3, 4]. Enlargement of the heart cavities and surgical scars are the basis for the formation of complex macro-reentrant atrial flutter. Until now, there were only sporadical cases

*Correspondence: dlgang101@163.com
State Key Laboratory of Cardiovascular Disease, Cardiac Arrhythmia Center, Fuwai Hospital, National Center for Cardiovascular Diseases, Chinese Academy of Medical Sciences and Peking Union Medical College, Beijing, China

reporting the successful ablation of atrial flutter in ccTGA patients [5, 6].

Here, we report a case of successful ablation in a atrial flutter patient with congenital dextrocardia, ccTGA and aberrant left atrial appendage (LAA), the surgical history of atrial septal defect repair and morphological tricuspid valvuloplasty also make the mechanism of arrhythmia more complicated and confusing. A combination of

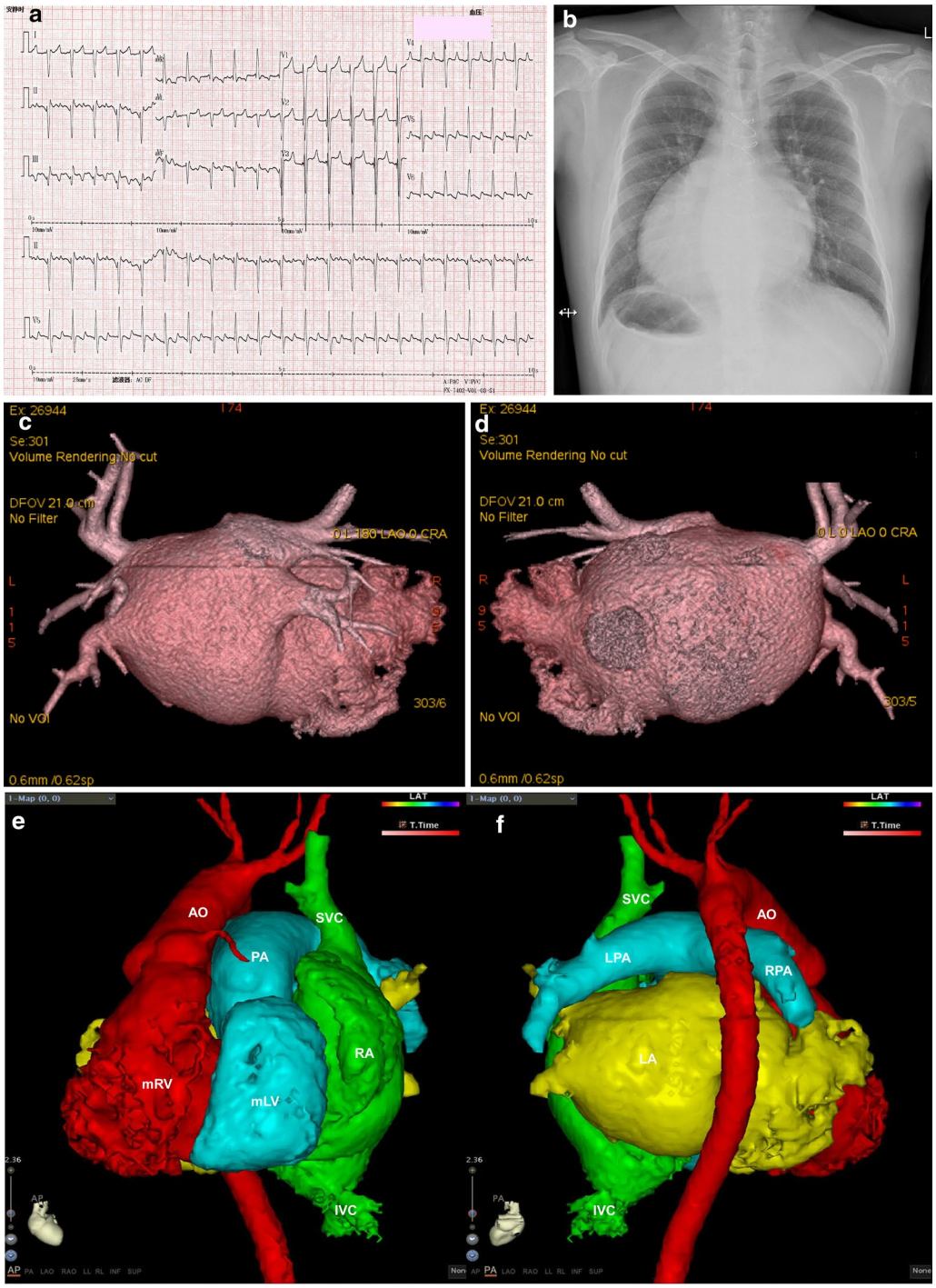


**Fig. 1** Electrocardiograph and imaging data. **a** Electrocardiograph; **b** chest X-ray; **c**, **d** reconstructed geometric structure of LA by contrast-enhanced computed tomography; **e**, **f** reconstructed 3-dimensional imaging of atriums and ventricles. *LA* left atrium, *RA* right atrium, *mRV* morphological right ventricle, *mLV* morphological left ventricle, *AO* aorta, *PA* pulmonary artery, *LPA* left pulmonary artery, *RPA* right pulmonary artery, *SVC* superior vena cava, *IVC* Inferior vena cava

high-density mapping and classic entrainment mapping is the key to successful ablation of the complex atrial flutter.

## Case presentation

A 36-year-old male with a history of dextrocardia, atrial septal defect, and ccTGA underwent atrial septal defect repair and morphological tricuspid valvuloplasty in 2014. However, several months later, he experienced a drug-refractory persistent atrial flutter and progressive deterioration of morphological right ventricle (mRV) function. The ejection fraction of mRV ranged from 47 to 54% during sinus rhythm and decreased to 28–42% during atrial flutter. Intermittently administration of amiodarone was used to treat atrial flutter. Electrocardiogram showed an atrial flutter at 130 beats/min with 2:1 atrioventricular conduction (Fig. 1a). A chest X-ray showed dextrocardia, left-sided hepatic contour, right-sided magenblase, and an enlarged cardio-thoracic ratio (Fig. 1b). Echocardiogram showed severe morphological tricuspid regurgitation with mRV ejection fraction of 35%. The diameters of right atrium (RA), left atrium (LA) and mRV end-diastolic diameter are 51, 54 and 73 mm, respectively.

Before electrophysiological study (EPS), contrast-enhanced computed tomography was performed to demonstrate the anatomical structure of the abnormal heart. Reconstructed geometric structure of LA revealed an unusually huge LAA (Fig. 1c, d). We also used CARTO-SYNC™ to reconstruct the 3-dimensional imaging of atriums and ventricles and conform the spatial relationship between them (Fig. 1e, f), which would be a useful guidance for atrial septal puncture and EPS.

A decapolar steerable electrode catheter was positioned within coronary sinus and a hexapolar electrode catheter was placed in morphologically left ventricular (mLV) separately. The intracardial ECG revealed an atrial flutter with a cycle length (CL) of 257 ms. A Penta-Ray catheter (Biosense Webster, Inc., Diamond Bar, CA, USA) was used to perform high-density mapping of the RA under the guidance of the Carto 3 system (Biosense Webster, Inc., Diamond Bar, CA, USA). The activation mapping revealed a passive activation pattern from LA to RA, the postpacing interval (PPI) after entrainment at coronary sinus (CS) ostium and free atrial wall were 245 ms and 423 ms, respectively, which means the reentrant circuit comes from LA rather than the RA.

Therefore, we performed high-density mapping of the LA after interatrial septal puncture through the surgical patch [7]. As vividly showed in activation mapping (Fig. 2a, b), two reentry circuit loops were located around the morphological tricuspid annulus (functional mitral annulus) and local area behind aberrant LAA, respectively. Propagation mapping and RIPPLE mapping show the activation sequence of two reentry circuit loops vividly (Additional files 1, 2, 3, 4). The two reentry circuit loops were overlapped in inferior area behind LAA (close to 6' clock of tricuspid annulus). The major tachycardia circuit consecutively rotated around the tricuspid annulus in a counterclockwise direction and had a proximal to distal activation pattern in the coronary sinus. The PPI after entrainment at the 6' clock, 12' clock of morphological tricuspid annulus and posterior wall were 271 ms, 255 ms and 275 ms, respectively.

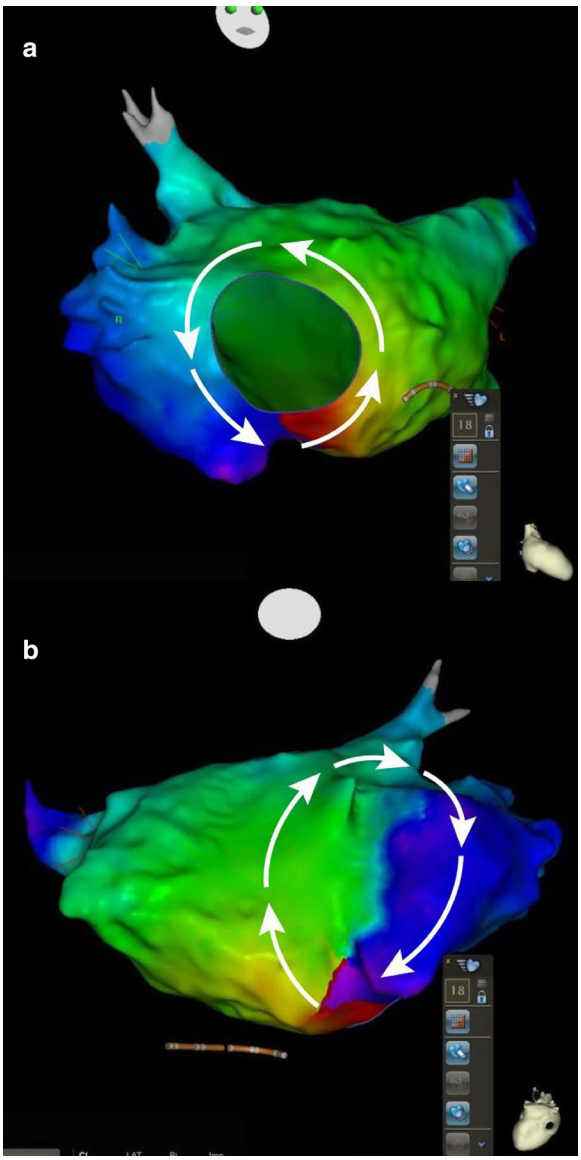


**Fig. 2** High-density mapping and entrainment of LA. **a** High-density mapping of the LA showing the major tachycardia circuit located around the anatomic tricuspid annulus (functional mitral annulus). **b** Second tachycardia circuit located in local area behind aberrant left atrial appendage

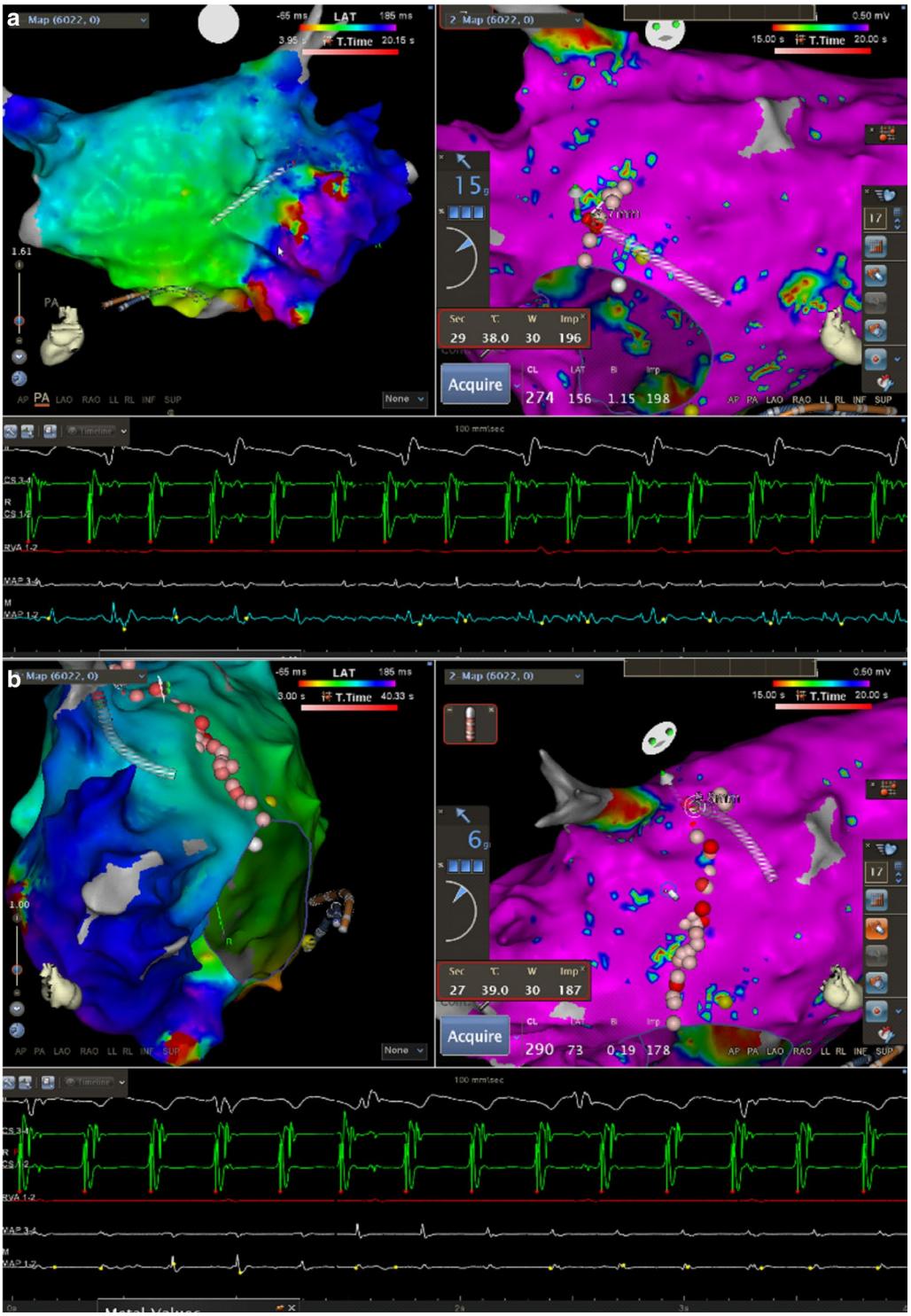


**Fig. 3** The first ablation line. **a** The first ablation line was performed from 12′ clock of tricuspid annulus to right superior pulmonary vein (RSPV). During ablation of this line, CL of atrial flutter prolonged from 260 to 275 ms. **b** CL of atrial flutter increased to 290 ms but tachycardia did not terminate when the first ablation line accomplished

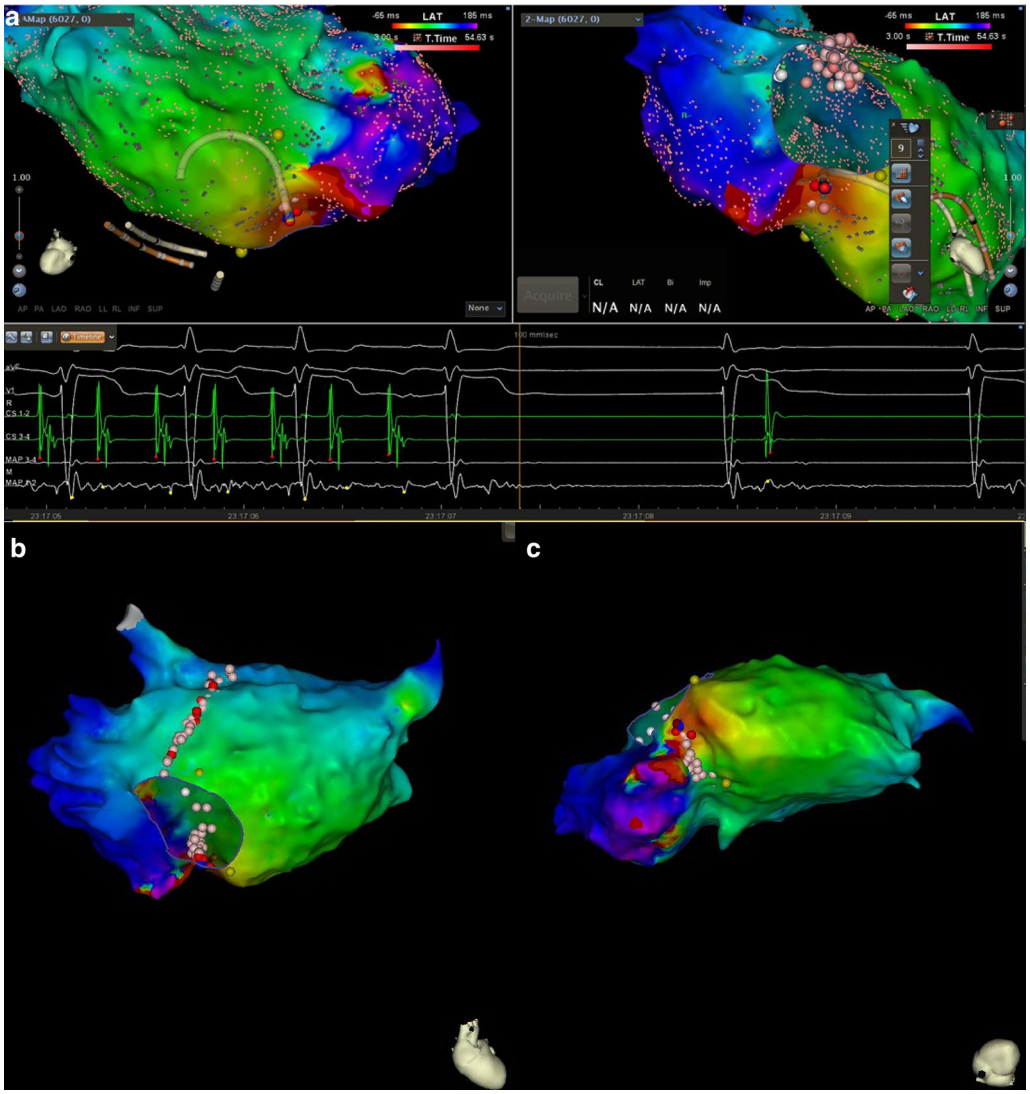


**Fig. 4** Complete ablation lines. **a** Atrial flutter was terminated when second ablation line from inferior endocardium of left atrial appendage to 6' clock of morphological tricuspid annulus accomplished. **b** The first ablation line. **c** The second ablation line

Since the aberrant LAA almost occupied the entire atrial free wall in this patient, it is difficult to perform conventional mitral isthmus line to connect the morphological tricuspid annulus and the ostium of the right inferior pulmonary vein. The first ablation line we performed was from 12' clock of morphological tricuspid annulus to right superior pulmonary vein (RSPV). During ablation of this line, CL of atrial flutter prolonged from 260 to 275 ms, and when this ablation line accomplished, CL increased to 290 ms but tachycardia did not stop (Fig. 3a, b). Entrainment mapping at a pacing cycle length of 270 ms demonstrated a PPI of 351 ms in anterior wall (close to 1' clock of tricuspid annulus) and 282 ms in posterior wall (close to 6' clock of tricuspid annulus), respectively. Entrainment from posterior wall also demonstrates a good stimulus-to-p wave interval (99 ms, S-P/AFLCL = 0.34) with concealed fusion, confirming this as the critical isthmus of the atrial flutter. Therefore, we performed second ablation line carefully from right inferior pulmonary vein to 6' clock of morphological tricuspid annulus, which was also the overlapped area of two reentry circuit loops, and terminated the tachycardia (Fig. 4a). Two ablation lines were illustrated in Fig. 4b/c and sinus rhythm was shown in ECG after ablation (Fig. 5). We confirmed the complete conduction block by activation map along the TA and by differential pacing from each end of the ablation lines.

The patient reported no tachycardia episodes during the 8-month follow-up after the procedure.

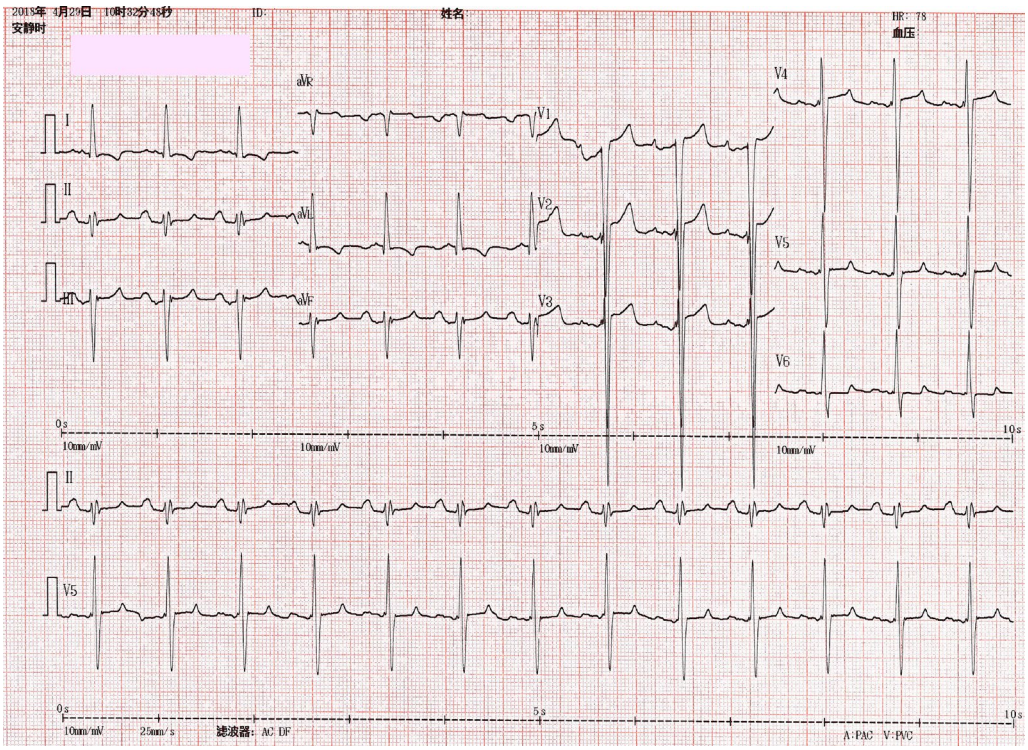


**Fig. 5** Electrocardiograph after ablation

Echocardiogram showed functional left ventricular ejection fraction increased to 49% and functional left ventricular end-diastolic diameter decreased to 60 mm at the 8-month follow-up visit.

## Discussion and conclusions

Due to the aberrance of anatomy and the complexity of procedures, only few cases reported radiofrequency ablation therapy for the arrhythmias in ccTGA patients. Our case report reveals several potential experiences in electrophysiological procedure in complex CHD patients: (1) previous reconstruction of the 3-dimensional imaging of atriums before EP test can be a useful guidance for atrial septal puncture and electrophysiological mapping in complex CHD. (2) High-density mapping makes the mechanism of arrhythmia in complex CHD more clear. (3) The combination of high-density mapping and entrainment mapping can simplify the design of ablation strategy.

High-density mapping technology has been developing rapidly in recent years. As for the endocardial mapping in this patient, anatomical and electrogram data from the atrium were automatically collected with rapid, high-density acquisition facilitated by the use of the system in conjunction with the PentaRay catheter. Activation map and voltage map were created with 3156 points in right atrium and 6228 points in left atrium. Previous studies have reported the advantages and effectiveness of high-density mapping in the mapping and ablation of complex arrhythmias [8–10]. It is essential to comprehensively combine activation map, voltage map and entrainments in the ablation strategy design. In this case, we not only performed the electroanatomic mapping of the atriums, but also used procedure of entrainments to confirm the location of atrial flutter more precisely and reliably. We also found the overlapped area of two reentry circuit loops which maybe the critical isthmus ("red" to "purple" in activation map and confirmed by concealed entrainment). We did not perform first ablation line in this area because of the safety concern about perforation when ablation across the large LAA, and the traditional ablation line from RIPV to morphological tricuspid annulus in this case is also difficult to achieve. Although the first ablation line did not terminate the tachycardia, it did increase the CL of atrial flutter. Entrainments after accomplishment of the first ablation line further verified the overlapped area of two reentry circuit loops still in the critical isthmus. The second ablation line terminated the atrial flutter, which might confirm the mechanism we presented.

We first considered the mechanism of atrial flutter is left atrial dual-loop reentry. The LAA-tricuspid valve isthmus constitutes the common pathway between both reentrant loops, this double-loop reentry. However, another possible explanation is only peri-tricuspid annulus atrial flutter. The first ablation line did not block the circuit but slow down the conduction. The prolonged PPI in anterior wall of TVA might due to rate-dependent decremental conduction across the first ablation line. No matter what mechanism (dual-loop reentry or peri-tricuspid annulus), the bidirectional conduction block across the LAA-tricuspid valve isthmus is key to prevent the long-term recurrence of atrial flutter.

In summary, we describe a complex atrial flutter in a patient with ccTGA and aberrant LAA. The successful procedure outlines the importance of realizing the relationship of atriums pre- and intraprocedural by explicit 3-dimensional reconstruction imaging. In the treatment of the patients with complex CHD accompanied by rapid arrhythmia, the combination of high-density mapping and entrainment mapping can be simpler, safer and more effective.

## Supplementary information

**Supplementary information** accompanies this paper at https://doi.org/10.1186/s42444-019-0004-1.

**Additional file 1.** Propagation mapping at anteroposterior view.

**Additional file 2.** Propagation mapping at posteroanterior view.

**Additional file 3.** RIPPLE mapping at anteroposterior view.

**Additional file 4.** RIPPLE mapping at posteroanterior view.

### Abbreviations

ccTGA: congenitally corrected transposition of great arteries; CHD: congenital heart disease; LAA: left atrial appendage; mRV: morphological right ventricle; RA: right atrium; LA: left atrium; EPS: electrophysiological study; mLV: morphologically left ventricular; CL: cycle length; PPI: postpacing interval; CS: coronary sinus; RSPV: right superior pulmonary vein.

### Acknowledgements

The authors would like to thank Dr. Win-kuang Shen for his helpful advice and comments. We also thank Hanxu Niu and Xiaomang Wang for their technical support in Carto electrophysiological mapping.

### Authors' contributions

LD is the main operator of this case; FH is the first aid and drafted this article; EL is the second aid; and LZ made a critical revision of article. All the authors read and approved the final manuscript.

### Funding

Not applicable.

### Availability of data and materials

All data generated or analyzed during this study are included in this published article.

### Ethics approval and consent to participate

This case report was approved by Institutional Ethics Committee for Biomedical Research of Fuwai Hospital. Proper written informed consent was obtained from this patient.

### Consent for publication

Consent for publication has been obtained from this patient.

### Competing interests

The authors declare that they have no competing interests.

Received: 13 February 2019 Accepted: 20 June 2019
Published online: 20 November 2019

### References

1. Warnes CA. Transposition of the great arteries. Circulation. 2006;114:2699–709.
2. Kutty S, Danford DA, Diller GP, Tutarel O. Contemporary management and outcomes in congenitally corrected transposition of the great arteries. Heart. 2018;104:1148–55.
3. Jacobs JP, Jacobs ML, Mavroudis C, Chai PJ, Tchervenkov CI, Lacour-Gayet FG, et al. Transposition of the great arteries: lessons learned about patterns of practice and outcomes from the congenital heart surgery database of the society of thoracic surgeons. World J Pediatr Congenit Heart Surg. 2011;2:19–31.
4. Said SM, Burkhart HM, Schaff HV, Dearani JA. Congenitally corrected transposition of great arteries: surgical options for the failing right ventricle and/or severe tricuspid regurgitation. World J Pediatr Congent Heart Surg. 2011;2:64–79.
5. Kalarus Z, Kowalski O, Lenarczyk R, Pruszkowska-Skrzep P, Pluta S, Zeifert B, et al. Radio-frequency ablation of arrhythmias following congenital heart surgery. Kardiol Pol. 2006;64:1343–8.
6. Palma EC, Raiszadeh F. Ablation of peri-"mitral" flutter in a patient with congenitally corrected transposition of great vessels and situs inversus. Pacing Clin Electrophysiol. 2012;35:e94–6.
7. Yao Y, Ding L, Chen W, Guo J, Bao J, Shi R, et al. The training and learning process of transseptal puncture using a modified technique. Europace. 2013;15:1784–90.
8. De Pooter J, El Haddad M, Wolf M, Phlips T, Van Heuverswyn F, Timmers L, Tavernier R, Knecht S, Vandekerckhove Y, Duytschaever M. Clinical assessment and comparison of annotation algorithms in high-density mapping of regular atrial tachycardias. J Cardiovasc Electrophysiol. 2018;29:177–85.
9. Maagh P, Christoph A, Dopp H, Mueller MS, Plehn G, Meissner A. High-density mapping in ventricular tachycardia ablation: a PentaRay((R)) study. Cardiol Res. 2017;8:293–303.
10. Segerson NM, Lynch B, Mozes J, Marks MM, Noonan DK, Gordon D, et al. High density mapping and ablation of concealed low voltage activity within pulmonary vein antra results in improved freedom from atrial fibrillation compared to pulmonary vein isolation alone. Heart Rhythm. 2018;15:1158–64.

## Publisher's Note